Electric Power Systems Research 201 (2021) 107499

Contents lists available at ScienceDirect

Electric Power Systems Research

journal homepage: www.elsevier.com/locate/epsr

# Optimal scheduling of a reconfigurable active distribution network with multiple autonomous microgrids

Houman Bastami, Mahmoud Reza Shakarami *, Meysam Doostizadeh

*Faculty of Engineering, Lorestan University, 5km Tehran Road, Khorramabad, Lorestan 68151-44316, Iran*

ARTICLE INFO

*Keywords:*
Active distribution network
Decentralized scheduling
Multiple autonomous microgrids
Reconfiguration
Information privacy

ABSTRACT

In this paper, a decentralized framework for optimal scheduling of a reconfigurable Active Distribution Network (ADN) is proposed that preserves the autonomy and information privacy of all the agents, i.e., the distribution system and microgrid's operators. In the proposed framework, the scheduling problem is decomposed to a certain number of Local Scheduling Models (LSMs), in such a way that each agent can independently schedule its network. In the proposed LSM, all technical constraints such as AC load flow equations, and radiality constraints are respected. Also, a Multi-Level Analytical Target Cascading (MLATC)-based method is proposed to coordinate the scheduling results of the LSMs. In this framework, by introducing new auxiliary variables, the shared variables that couple the LSMs are limited to only three types. Using the proposed framework, the optimal configuration of the ADN and the operational scheduling of agents are simultaneously calculated. Since all technical constraints are modeled in the proposed LSM, the results are both economic and feasible. To assess the optimality and effectiveness of the proposed method, several simulations are carried on the modified IEEE 33-bus and IEEE 123-bus distribution test systems. Moreover, the results are compared with the centralized approach to validate the optimality of the solution.

## 1. Introduction

By modernizing distribution system infrastructure and high penetration of Distributed Energy Resources (DERs), distribution networks are facing a transition from a central structure to a distributed one [1]. Accordingly, the interconnection of multiple Microgrids (MGs) has appeared as a new design to reach more economic benefits, reliable energy supply, lower operational costs in Active Distribution Networks (ADNs) [2]. However, autonomous MGs are pursuing their interests and want to minimize their scheduling cost. MGs can be encouraged to join energy trading only if their benefits are not less than the ones without cooperation [3]. To achieve profit maximization for autonomous MGs, an effective method is required to perform energy scheduling and trading between MGs. Several studies such as [4–6] present centralized [5–7]frameworks for optimal energy trading among MGs. In the centralized frameworks, all MGs should send the whole of their local network data, such as loads and DERs data, to a central coordinator. This coordinator schedules ADN centrally and sends optimal scheduling results to the agents. Although some centralized approaches such as [7] can achieve optimal scheduling, it is unable to preserve the information privacy and independence of the agents [8].

To overcome these deficiencies, recent studies such as [9–15] apply decentralized and distributed methods. In these approaches, all agents within an ADN schedule their DERs independently, and only a limited data, named as shared variables are communicated among them. However, in distributed approaches, such as [12,13], there are no direct communication links between the agents, and they are coordinated through a central coordinator [15]. Unlike distributed approaches, decentralized methods such as [8,11,14] have not a central coordinator, and the agents directly communicate with each other [15].

In [10], a decentralized model for scheduling of an ADN comprising several interconnected agents is presented, and an Alternating Direction Method of Multipliers (ADMM) is utilized to coordinate them in a decentralized style. A hierarchical optimization algorithm based on the system of systems concept is proposed in [9], that both Distribution Network (DN) and MGs are managed independently. A fully distributed ADMM-based method for reactive power optimization of the ADN is proposed in [11]. In [10], four types of shared variables, i.e. transacted

* Corresponding author.
*E-mail addresses:* bastami.hu@fe.lu.ac.ir (H. Bastami), shakarami.mr@lu.ac.ir (M.R. Shakarami), doostizadeh.m@lu.ac.ir (M. Doostizadeh).

https://doi.org/10.1016/j.epsr.2021.107499
Received 4 January 2021; Received in revised form 29 July 2021; Accepted 1 August 2021
Available online 19 August 2021

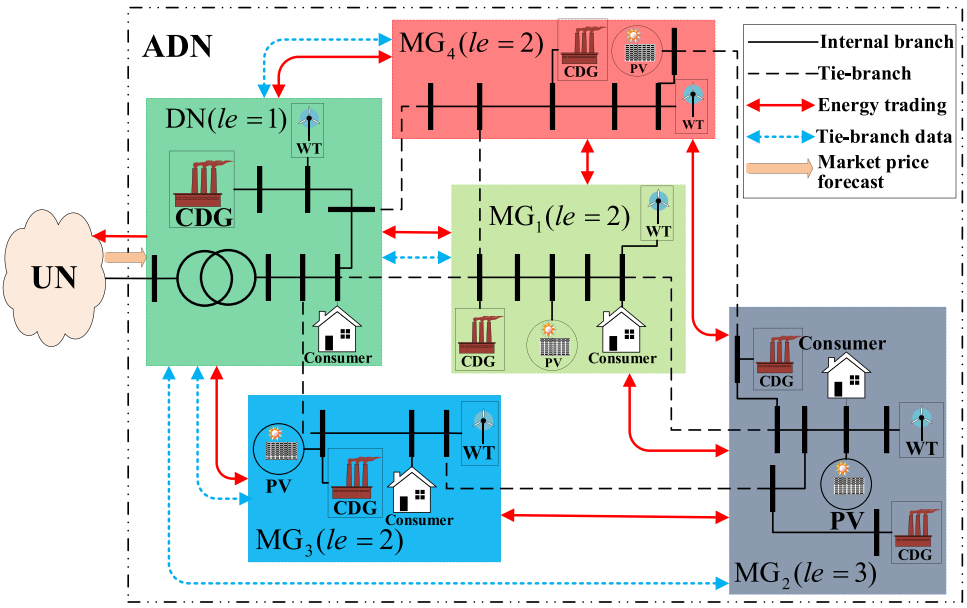


**Fig. 1.** A reconfigurable ADN with 5 autonomous agents.

active and reactive power, current of tie branches, and voltage of border buses are exchanged between the agents to coordinate them. In some of the decentralized approaches such as [11], the neighboring agents must exchange the injected active and reactive power to their border buses, these data are private and the privacy of the agents is somewhat violated. Also, some decentralized approaches such as [11] and [10], require a lot of exchanged data.

In addition to scheduling of DERs in ADNs, the configuration of an ADN affects transactions between the agents, voltage profile [16], and can decrease the system operation cost [17]. To do so, the topology of ADNs can be optimized through Remotely Controlled Switches (RCSs) during short-term operation. In this regard, optimal day-ahead scheduling of RCSs and DERs is presented in [18] to minimize the power losses and the number of switching actions using a hybrid Particle Swarm Optimization (PSO)-based approach. Also, in [19], the distribution network reconfiguration problem is solved using a genetic algorithm with varying populations. In [20], a fast strategy is proposed which enhances solution speed and quality of the distribution system reconfiguration problem by selecting the initial candidate solutions. To minimize distribution network power losses, a reconfiguration technique based on the binary PSO is proposed in [21]. A stochastic optimal scheduling method for reconfigurable smart MGs is presented in [22] to maximize the total profits. Also, a centralized approach based on the PSO with time-varying acceleration coefficients is used to schedule whole MGs. A centralized approach for simultaneous optimization of both network reconfiguration and reactive power dispatch is presented in [23] to decreasing power losses and voltage violations. In [24], an optimal operational scheduling framework based on the genetic algorithm is proposed to minimize the day-ahead total operation cost of the ADN. The optimal hourly topology of the network for the scheduling time horizon is determined as well. A stochastic mixed-integer linear programming model is formulated in [25] to perform dynamic network reconfiguration from the Distribution System Operator (DSO)'s point of view. In [17], an optimization model based on the mixed-integer second-order cone programming problem is proposed for minimizing the operational cost of a reconfigurable ADN. However, the privacy of DERs owners is not considered and only the transaction between the ADN and its Upstream Network (UN) is scheduled.

Although the above-centralized approaches may reach the optimal solution, they are not applicable for multi-agent ADNs due to neglecting the autonomy and privacy of the agents. Accordingly, a non-cooperative two-person-based Stackelberg game theory framework for scheduling of a reconfigurable ADN under the electricity market is formulated in [26]. In this study, the DSO, as the leader of the game, schedules the ADN to reduce the operational cost. Then, the owners of DGs, as followers, try to maximize their profits from DG investment, based on the configuration of the network. However, the privacy of the agents, i.e., the owners of DGs, is not considered and DSO should access the technical information of all DGs. A one-leader multi-follower-type bi-level optimization model is proposed in [12] that minimizes the operation cost of DSO and maximizes the profit of MGs, simultaneously. However, the information privacy of the MGs is not considered in this model. Ref. [13] proposes a bi-level programming framework to coordinate multi-MG energy trading and the operation of reconfigurable ADNs. At the lower level, MGs participate in a local transactive energy trading market. Then, nodal equivalent loads are sent to the DSO at the upper level to reconfigure the distribution network. The updated topology which satisfies total technical constraints is sent back to the lower level in an iterative process. However, network constraints of MGs are neglected in this approach, and MGs are only modeled as dispatchable resources connecting to the distribution system.

In the above researches, the optimal configuration of an ADN is centrally determined by DSO, and the physical constraints of the ADN are not modeled in the Local Scheduling Model (LSM) of the MGs. Therefore, the MGs cannot affect their connections to other agents, directly.

This paper proposes a novel decentralized framework for optimal scheduling of a reconfigurable ADN that preserves the autonomy and information privacy of the agents. In this approach, short-term scheduling of the agents and reconfiguration of the ADN is integrated as a novel decentralized optimization problem. Moreover, the network constraints of the ADN are modeled in a decentralized style and added to the LSM of each agent. Also, a new Multi-Level Analytical Target Cascading (MLATC)-based method is developed to coordinate the scheduling of the agents. Accordingly, the main contributions of this paper are as follow:

(1) A decentralized framework for optimal scheduling of a reconfigurable ADN is proposed that preserves the autonomy and information privacy of all the agents, i.e., DSO and MG operators.
(2) The scheduling problem of whole the ADN is decomposed to a certain number of LSMs. Accordingly, each agent can independently schedule its network.

(3) All technical constraints such as AC load flow equations, radiality constraints, nodal voltage limitation, and technical constraints of DERs are modeled into the agent's LSM. So, the optimal configuration of the ADN and the operational scheduling of agents are simultaneously calculated.
(4) An MLATC-based method is proposed to coordinate the scheduling results of the LSMs.
(5) By introducing new auxiliary variables, the number of shared variables that couple the LSMs is limited to only three types. Accordingly, the proposed decentralized method has the least data sharing.

The rest of this paper is organized as follows. The structure of a reconfigurable ADN with multiple MGs is described in section 2. The proposed LSM is presented in section 3. The details of the proposed MLATC are provided in section 4. In section 5, the simulation results on two test systems are presented. Finally, section 6 concludes the paper.

## 2. A reconfigurable ADN with multiple MGs

A modern reconfigurable ADN with 5 autonomous agents, i.e., DN and $MG_1$ to $MG_4$ is shown in Fig. 1. Each agent contains local consumers and DERs, such as Controllable Distributed Generators (CDGs), Wind Turbines (WTs), and Photovoltaics (PVs). These agents are connected via tie branches to each other, and they can exchange active and reactive power. In this figure, 7 tie branches are plotted by black dashed lines. To preserve the radiality of the ADN, only 4 of these tie branches should be in service, simultaneously.

The configuration of the ADN is determined based on the optimal transaction between the agents in a decentralized style. In this framework, each agent locally operates its network and broadcasts the results of its shared variables to its neighbors. As depicted in Fig. 1, only limited data, named energy trading and tie branches data, are shared among the agents. Note that, energy trading data, i.e., transacted active and reactive power, are shared between two neighboring agents, and tie-branch data, i.e., receiving end voltage of tie-branch multiplied by the status of the tie-branch, is only shared between DN and each of two agents that are connected to that tie-branch.

To coordinate agents, a decentralized framework based on MLATC is proposed. The proposed decentralized approach has a hierarchical structure, in which the agents must be scheduled in order of their levels and sublevels. In this structure, the DN is considered as level one ($le = 1$). The agents which are connected directly to the DN are considered as level two ($le = 2$). In the same way, other levels are defined. For example, in Fig. 1, $MG_1$, $MG_3$, and $MG_4$ are placed in level two, and the level of $MG_2$ is three. So, this ADN has three levels ($N^{le} = 3$). Note that, the agents at a certain level must be sequentially scheduled based on their sublevels, which are defined based on an arbitrary consecutive order. For example, if the sublevels of $MG_1$, $MG_3$, and $MG_4$ are respectively assumed to be $sl = 1, 2, 3$, these agents follow the same priority to solve their LSM.

Coordination between agents is achieved through an iterative process. The details of the proposed MLATC-based framework are represented in section 4. In the following, the proposed LSM of each agent is presented in a general format.

## 3. The proposed LSM

In this paper, it is assumed that each agent aims to minimize its operation cost. So, the LSM of agent $a$ can be represented as follows:

$$\min Cost^a_{to} = Cost^a_{CDG} + Cost^a_{UN} + Cost^a_{SW} \quad subject to (5) - (26) \tag{1}$$

where $Cost^a_{to}$ represents the total cost of agent $a$ in scheduling horizon $T$. Note that, in this paper, the private parameters and variables associated with the agent $a$ are specified with superscript $a$. $Cost^a_{CDG}$ and $Cost^a_{UN}$ are respectively total generation cost of CDGs, and the cost of purchasing power from the UN, which are defined in (2) and (3). Finally, $Cost^a_{SW}$ is the sum of switching cost of the tie branches that is defined in (4).

$$Cost^a_{CDG} = \tau \sum_{t\in T} \sum_{g\in N^a_{CDG}} \left( a^a_g \times \left( Pg^a_{t,g} \right)^2 + b^a_g \times Pg^a_{t,g} + c^a_g \right) \tag{2}$$

$$Cost^a_{UN} = \tau \sum_{t\in T} \left( Pun^a_t \times \lambda_t \right) \tag{3}$$

$Pg^a_{t,g}$ is the active power generation of CDG $g$ at time interval $t$; $a^a_g$, $b^a_g$, and $c^a_g$ are the cost coefficients of CDG $g$; $N^a_{CDG}$ is the set of CDGs which are owned by agent $a$; $\lambda_t$ is the forecasted wholesale market price at time interval $t$; $\tau$ is the length of each time interval, and $Pun^a_t$ is the imported power from the UN at time interval $t$. Note that, the generation cost of PVs and WTs is assumed to be zero [8].

$$Cost^a_{SW} = c_{sw} \sum_{t\in T} \sum_{kj\in N^a_{tb}} \varphi^a_{t,kj} \tag{4}$$

$c_{sw}$ is the cost of switching action, and $\varphi^a_{t,kj}$ is a binary variable that shows the switching action of tie-branch $kj$ at time interval $t$. If the statuses of tie-branch $kj$ in both time intervals $t-1$ and $t$ are the same, then $\varphi^a_{t,kj} = 0$; otherwise $\varphi^a_{t,kj} = 1$. $N^a_{tb}$ is the set of the tie branches that are connected to agent $a$.

Active, reactive, and apparent powers generation of CDGs are limited by (5)–(7), respectively.

$$Pg^a_{\min,g} \le Pg^a_{t,g} \le Pg^a_{\max,g} \ \forall g \in N^a_{CDG}, \ \forall t \in T \tag{5}$$

$$Qg^a_{\min,g} \le Qg^a_{t,g} \le Qg^a_{\max,g} \ \forall g \in N^a_{CDG}, \ \forall t \in T \tag{6}$$

$$Pg^{a\ 2}_{t,g} + Qg^{a\ 2}_{t,g} \le Sg^{a\ 2}_{\max,g} \forall g \in N^a_{CDG}, \ \forall t \in T \tag{7}$$

$Qg^a_{t,g}$ is reactive power generation of CDG $g$ at time interval $t$. $Pg^a_{\min,g}$ and $Pg^a_{\max,g}$ are the minimum and maximum active power generation of CDG $g$. Also, $Qg^a_{\min,g}$ and $Qg^a_{\max,g}$ are the minimum and maximum reactive power generation of CDG $g$, and $Sg^a_{\max,g}$ is the maximum capacity of apparent power generation of CDG $g$.

Constraints (8) and (9) represent downward and upward ramping capability limits of CDGs during the scheduling horizon, respectively.

$$Pg^a_{t-1,g} - Pg^a_{t,g} \le Rdn^a_g \times \tau \ \forall g \in N^a_{CDG}, \ \forall t \in T \tag{8}$$

$$Pg^a_{t,g} - Pg^a_{t-1,g} \le Rup^a_g \times \tau \ \forall g \in N^a_{CDG}, \ \forall t \in T \tag{9}$$

$Rdn^a_g$ and $Rup^a_g$ are the maximum down and up ramp rate of CDG $g$, respectively.

To model AC load flow constraints in a reconfigurable ADN in a decentralized style, the *distflow* model [27] is developed as presented in (10)–(26). Note that, the network, DERs, and loads are assumed to be balanced, here. Like the *distflow* model, squared current ($I_{t,kj}$), injected active and reactive power ($Pf_{t,kj}$, $Qf_{t,kj}$) of lines, along with the squared voltage magnitude ($v_{t,j}$) of buses are considered as decision variables. A binary variable ($Sb_{t,kj}$) is introduced to determine the status of the line connecting bus $k$ to $j$. $Sb_{t,kj} = 1$ if line $kj$ at time interval $t$ is in service; otherwise, $Sb_{t,kj} = 0$. Since the internal configuration of the agent's network is assumed to be fixed, the internal branches of each agent must be in service for all time intervals, as defined in (10).

$$Sb_{t,kj} = 1 \ \forall kj \in N^a_{ib}, \forall t \in T \tag{10}$$

$N^a_{ib}$ is the set of all internal branches in the network of agent $a$. To apply load flow formulation on a reconfigurable ADN, we encounter a meshed network due to the existence of the tie branches. Therefore, each bus may have more than one upstream bus.

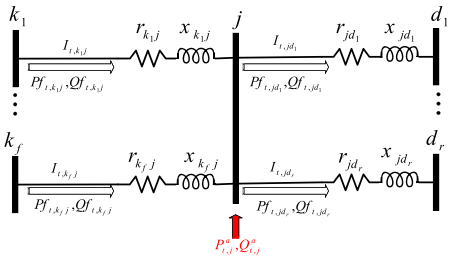

**Fig. 2.** Load flow of bus $j$ operated by agent $a$. (For interpretation of the references to color in this figure, the reader is referred to the web version of this article.).

As depicted in Fig. 2, buses $k_1$ to $k_f$ are the upstream buses of bus $j$ (set $N_j^{Up}$) and it is assumed that they inject power to bus $j$ through lines $k_1j$ to $k_fj$, respectively. Also, buses $d_1$ to $d_r$ are downstream buses of bus $j$ (set $N_j^{Dn}$), and receive power from bus $j$ via lines $jd_1$ to $jd_r$. Accordingly, the effect of multiple upstream buses is represented by $\sum_{k\in N_j^{Up}}(Pf_{t,kj}-r_{kj}I_{t,kj})$ and $\sum_{k\in N_j^{Up}}(Qf_{t,kj}-x_{kj}I_{t,kj})$ in nodal power balance Eqs. (11) and (12).

$$\sum_{d\in N_j^{Dn}} Pf_{t,jd} - \sum_{k\in N_j^{Up}}\left(Pf_{t,kj}-r_{kj}I_{t,kj}\right) = P_{t,j}^{a}\,\forall j\in N_{bus}^{a},\forall t\in T \tag{11}$$

$$\sum_{d\in N_j^{Dn}} Qf_{t,jd} - \sum_{k\in N_j^{Up}}\left(Qf_{t,kj}-x_{kj}I_{t,kj}\right) = Q_{t,j}^{a}\;\forall j\in N_{bus}^{a},\forall t\in T \tag{12}$$

$r_{kj}$ and $x_{kj}$ are the resistance and reactance of line $kj$, respectively. $N_{bus}^{a}$ is the set of buses in the ADN which are owned by agent $a$. $P_{t,j}^{a}$ and $Q_{t,j}^{a}$ are respectively the net injected active and reactive power to bus $j$ at time interval $t$ determined by (13) and (14). Note that, line variables may be local or shared whether they are associated with internal branches or tie branches, while $P_{t,j}^{a}$ and $Q_{t,j}^{a}$ are local decision variables and are highlighted by red color in Fig. 2.

$$P_{t,j}^{a} = \sum_{g\in N_{CDG,j}^{a}} Pg_{t,g}^{a} + \sum_{w\in N_{WT,j}^{a}} WT_{t,w}^{a} + \sum_{p\in N_{PV,j}^{a}} PV_{t,p}^{a} + Pun_{t,j}^{a} - Pl_{t,j}^{a}\;\forall j\in N_{bus}^{a},\forall t\in T \tag{13}$$

$$Q_{t,j}^{a} = \sum_{g\in N_{CDG,j}^{a}} Qg_{t,g}^{a} + Qun_{t,j}^{a} - Ql_{t,j}^{a}\;\forall j\in N_{bus}^{a},\forall t\in T \tag{14}$$

$WT_{t,w}^{a}$ and $PV_{t,p}^{a}$ are forecasted generation of WT $w$ and PV $p$ in time interval $t$. $N_{CDG,j}^{a}$, $N_{WT,j}^{a}$, and $N_{PV,j}^{a}$ are the set of CDGs, PVs, and WTs locating at bus $j$ and operated by agent $a$, respectively. $Pl_{t,j}^{a}$ and $Ql_{t,j}^{a}$ are respectively active and reactive power demand of bus $j$ at time interval $t$. $Qun_{t,j}^{a}$ is the imported reactive power to bus $j$ from the UN. Constraint (15) maintains the squared magnitude voltage of buses within its allowable limits ($[v_{min},v_{max}]$). The squared magnitude voltage of the slack bus is represented by (16).

$$v_{min}^{\,2} \le v_{t,j} \le v_{max}^{\,2}\;\forall j\in\left\{N_{bor}^{a},N_{bus}^{a}\right\},\;\forall t\in T \tag{15}$$

$$v_{t,j} = v_{sl}^{\,2}\;\forall j\in N_{sl},\;\forall t\in T \tag{16}$$

$N_{sl}$ is the set of the slack bus and $v_{sl}$ is the voltage magnitude of the slack bus. $N_{bor}^{a}$ is the set of border buses that are connected to agent $a$ through tie branches. An auxiliary variable named *voltage status* ($vs_{t,kj}$) is defined to represent the squared voltage magnitude of the receiving end of tie-branch $kj$. Accordingly, if tie-branch $kj$ is in service, i.e., $Sb_{t,kj}=1$, (17) bounds $vs_{t,kj}$ within its allowable limits; otherwise, $vs_{t,kj}=0$. Eq. (18) relates $vs_{t,kj}$ to $v_{t,j}$.

$$\left(v_{min}^{\,2}\times Sb_{t,kj}\right) \le vs_{t,kj} \le \left(v_{max}^{\,2}\times Sb_{t,kj}\right)\;\forall kj\in N_{lin}^{ADN},\;\forall t\in T \tag{17}$$

$$\left(vs_{t,kj}+v_{min}^{\,2}\times\left(1-Sb_{t,kj}\right)\right) \le v_{t,j} \le \left(vs_{t,kj}+v_{max}^{\,2}\times\left(1-Sb_{t,kj}\right)\right)\;\forall kj\in N_{lin}^{ADN},\;\forall t\in T \tag{18}$$

$N_{lin}^{ADN}$ is the set of all lines in the ADN (including both internal and tie branches). The power flow relation between bus $j$ and its upstream bus $k$ is formulated as follows:

$$-M\times\left(1-Sb_{t,kj}\right) \le v_{t,k}-v_{t,j}-2\left(r_{kj}Pf_{t,kj}+x_{kj}Qf_{t,kj}\right)+\left(\left(r_{kj}\right)^{2}+\left(x_{kj}\right)^{2}\right)I_{t,kj} \le M\times\left(1-Sb_{t,kj}\right)\;\forall kj\in N_{lin}^{a},\forall t\in T \tag{19}$$

where $M$ is a big number. According to (19), when $Sb_{t,kj}=1$ the Ohm law should be considered for branch $kj$, otherwise there is no relation between two voltages $v_{t,k}$ and $v_{t,j}$.

Eq. (20) shows the conic relaxation of the branch flow equation [14].

$$\left\| \begin{matrix} 2Pf_{t,kj} \\ 2Qf_{t,kj} \\ v_{t,k}-I_{t,kj} \end{matrix} \right\|_2 \le v_{t,k}+I_{t,kj}\;\forall kj\in N_{lin}^{a},\forall t\in T \tag{20}$$

Inequalities (21) and (22) have respectively bounded squared current magnitude and apparent power flow in branch $kj$, for all time intervals.

$$0 \le I_{t,kj} \le \left(I_{Max,kj}^{2}\times Sb_{t,kj}\right)\;\forall kj\in N_{lin}^{a},\forall t\in T \tag{21}$$

$$Pf_{t,kj}^{\,2}+Qf_{t,kj}^{\,2} \le Sf_{Max,kj}^{\,2}\times Sb_{t,kj}\forall kj\in N_{lin}^{a},\forall t\in T \tag{22}$$

$I_{max,kj}$ and $Sf_{max,kj}$ are respectively the maximum allowable current and apparent power of line $kj$.

Eq. (23) preserves the radiality of the system. To do so, the number of in-service tie branches in every possible loop must be less than the total number of tie branches in that loop. In other words, each loop should have at least one open tie-branch. To find all possible loops in a given network, a depth-first search-based approach in [28] is applied. To identify all the loops in a network, all tie branches are assumed to be in service. It is worth mentioning that the loop detection process is offline and takes place only once before the optimization. Therefore, radiality constraints can be easily modeled and the optimization problem becomes very fast and suitable for short-term operation.

$$\sum_{kj\in Lp_l} Sb_{t,kj} \le NL_l-1\;\forall l\in L,\forall t\in T \tag{23}$$

$L$ is the set of possible loops in the ADN and $l$ is the index of the loop. $Lp_l$ is the set of the tie branches in loop $l$, and $NL_l$ is the number of tie branches in $Lp_l$.

Constrain (24) limits the number of switching actions in the scheduling horizon $T$, where $N_{tb}^{a}$ is the set of tie branches connected to agent $a$ and $SW_{max}^{a}$ is the maximum allowed number of switching actions in the scheduling horizon $T$. If the status of tie-branch $kj$ at times $t-1$ ($Sb_{t-1,kj}$) and $t$ ($Sb_{t,kj}$) are different, $\varphi_{t,kj}^{a}$ is set to one according to (25) and (26) [29].

$$\sum_{kj\in N_{tb}^{a}} \varphi_{t,kj}^{a} \le SW_{max}^{a}\;\forall t\in T \tag{24}$$

$$Sb_{t,kj}-Sb_{t-1,kj} \le \varphi_{t,kj}^{a}\;\forall kj\in N_{tb}^{a},\forall t\in T \tag{25}$$

$$Sb_{t-1,kj}-Sb_{t,kj} \le \varphi_{t,kj}^{a}\;\forall kj\in N_{tb}^{a},\forall t\in T \tag{26}$$

### 3.1. Shared variables

In the proposed LSM, $Pf_{t,kj}$, $Qf_{t,kj}$, $vs_{t,j}$, $Sb_{t,kj}$ and $I_{t,kj}$ are decision variables associated with each tie-branch that couple the LSMs of two neighboring agents. So, the remaining variables are locally determined. Since $vs_{t,kj}$ and $Sb_{t,kj}$ are interdependent through (17) and (18), $vs_{t,kj}$ can

be considered as a shared variable instead of both $vs_{t,kj}$ and $Sb_{t,kj}$. Also, two auxiliary variables $Pn_{t,kj}$ and $Qn_{t,kj}$ are introduced in (27) and (28) to be used as shared variables instead of $Pf_{t,kj}$, $Qf_{t,kj}$ and $I_{t,kj}$.

$$Pn_{t,kj} = Pf_{t,kj} - r_{kj}I_{t,kj} \ \forall kj \in N_{tb}^{a}, \forall t \in T \tag{27}$$

$$Qn_{t,kj} = Qf_{t,kj} - x_{kj}I_{t,kj} \ \forall kj \in N_{tb}^{a}, \forall t \in T \tag{28}$$

$Pn_{t,kj}$ and $Qn_{t,kj}$ respectively represent the net injected active and reactive power from bus $k$ to bus $j$ through line $kj$.

These substitutions reduce the number of shared variables to three and transform $Pf_{t,kj}$, $Qf_{t,kj}$, $vs_{t,j}$, $Sb_{t,kj}$ and $I_{t,kj}$ to local variables for all lines. Consequently, the shared variables associated with tie-branch $kj$ can be categorized into two vectors $PQ_{kj}$ and $vs_{kj}$ as follows:

$$PQ_{kj} = \left[Pn_{1,kj}, ..., Pn_{N,kj}, Qn_{1,kj}, ..., Qn_{N,kj}\right] \forall kj \in N_{tb}^{ADN} \tag{29}$$

$$vs_{kj} = \left[vs_{1,kj}, ..., vs_{N,kj}\right] \ \forall kj \in N_{tb}^{ADN} \tag{30}$$

where $PQ_{kj}$ and $vs_{kj}$ are respectively vectors with $2N$ and $N$ elements, which represent *energy trading* and *tie-branch data* of tie-branch $kj$ (as shown in Fig. 1). $N$ is the number of time intervals, and $N_{tb}^{ADN}$ is set of all tie branches in the ADN. To guarantee that all LSMs use the same value of shared variables while satisfying their local constraints, two following sets of consistency constraints are added to the LSM of agent $a$:

$$\begin{cases} PQ_{kj,z} = PQ_{kj,z}^{b} \ \forall kj \in N_{tb}^{a}, \forall z \in \{1, ..., 2N\} \\ vs_{kj,z} = vs_{kj,z}^{DN} \ \forall kj \in N_{tb}^{a}, \forall z \in \{1, ..., N\} \end{cases} \tag{31}$$

where vectors $vs_{kj}^{DN}$ and $PQ_{kj}^{b}$ are shared by DN and neighboring agent $b$, respectively. $z$ is the index of the vector's element.

## 4. The proposed MLATC

Adding the consistency constraint (31) to the LSM of agent $a$ requires a coordination strategy that effectively exchanges shared variables between the agents. To do so, in this paper, a coordination framework based on MLATC is proposed. In the proposed MLATC method, the entire ADN is modeled as a set of hierarchically connected agents. Agents in upper levels are hierarchically coupled to agents in lower levels via shared variables. From the upper-level agents' point of view, the shared variables are named as target variables, while lower-level agents consider the shared variables as response variables. Upper-level agents determine the values of target variables and share them with their lower-level agents. Then, the responses obtained by the lower-level agents determine how the targets are achieved [30]. Accordingly, the shared variables in consistency constraint (31) can be modeled as targets and response variables.

In the proposed MLATC method, the consistency constraint (31) is relaxed by adding a penalty term ($Penalty^{a,(it)}$) to the objective function of each agent. Accordingly, in the proposed MLATC framework, the objective of the LSM of agent $a$ is developed as follows:

$$\begin{aligned} &\min \left(\cos t_{to}^{a} + Penalty^{a,(it)}\right) \\ &\quad subjectto (5) - (26) \end{aligned} \tag{32}$$

Then coordination between agents is settled through a repetitive process of the MLATC. In each iteration of the process, i.e., iteration $it$, all the agents independently schedule their LSM, according to their level. First, the DN, at level 1 ($le = 1$) solves its LSM. Then, the agents that can be directly connected to the DN, schedule their LSM. These agents are considered as level 2 ($le = 2$). Likewise, the agents that can be directly connected to the agents in level 2 are considered as level 3 ($le = 3$). Similarly, the level of the remaining agents is determined. It is important to note that the level of agents in an ADN is determined before the process.

At each iteration of the repetitive process of the proposed MLATC framework, penalty term $Penalty^{a,(it)}$ is updated via (33).

$$\begin{aligned} Penalty^{a,(it)} &= \sum_{kj \in N_{tb}^{a}} \pi_{pq}^{a}\left(Cpq_{kj}^{a,(it)}\right) + \sum_{kj \in N_{as}^{a}} \pi_{vs}^{a}\left(Cvs_{kj}^{a,(it)}\right), N_{as}^{a} \\ &= \begin{cases} N_{tb}^{ADN} & a = DN \\ N_{tb}^{a} & otherwise \end{cases} \end{aligned} \tag{33}$$

Where $N_{as}^{a}$ for DN ($a = DN$) is equal to the set of all tie branches in the ADN ($N_{tb}^{ADN}$). Because the voltage status of all tie branches should be shared with the DN. While for other agents $N_{as}^{a}$ is equal to the set of tie branches that are connected to them ($N_{tb}^{a}$). $\pi_{pq}^{a}$ and $\pi_{vs}^{a}$ are augmented Lagrangian functions which are respectively defined as follows:

$$\pi_{pq}^{a}\left(Cpq_{kj}^{a,(it)}\right) = \left(Vpq_{kj}^{a,(it)}\right)^{T} \times Cpq_{kj}^{a,(it)} + \| \, Wpq_{kj}^{a,(it)} \circ Cpq_{kj}^{a,(it)} \, \|_{2}^{2} \tag{34}$$

$$\pi_{vs}^{a}\left(Cvs_{kj}^{a,(it)}\right) = \left(Vvs_{kj}^{a,(it)}\right)^{T} \times Cvs_{kj}^{a,(it)} + \| \, Wvs_{kj}^{a,(it)} \circ Cvs_{kj}^{a,(it)} \, \|_{2}^{2} \tag{35}$$

where $Vpq_{kj}^{a,(it)}$ and $Vvs_{kj}^{a,(it)}$ are Lagrangian multipliers that have $2N$ and $N$ elements, respectively. Also, $Wpq_{kj}^{a,(it)}$ and $Wvs_{kj}^{a,(it)}$ are respectively penalty weights with $2N$ and $N$ elements. These vectors are associated with shared variables of tie-branch $kj$ in the iteration $it$ and should be updated at each iteration of the proposed MLATC framework. $Cpq_{kj}^{a,(it)}$ and $Cvs_{kj}^{a,(it)}$ are the inconsistency between target and response variables which are defined in (36) and (37), respectively. Note that the $\circ$ symbol is applied to symbolize a term-by-term multiplication of vectors so that $[a_1, ..., a_n] \circ [b_1, ..., b_n] = [a_1 b_1, ..., a_n b_n]$. The $\times$ symbol represents matrix multiplication and $(A)^T$ denotes the transpose of matrix $A$.

$$Cpq_{kj}^{a,(it)} = \begin{cases} PQ_{kj}^{(h)} - PQ_{kj} & k \in N_{bus}^{a} \\ PQ_{kj} - PQ_{kj}^{(h)} & j \in N_{bus}^{a} \end{cases}, \quad h = \begin{cases} it - 1 & le_{kj}^{a} > le^{a} \\ it - 1 & le_{kj}^{a} = le^{a} \ \& \ sl_{kj}^{a} > sl_{a} \\ it & else \end{cases} \tag{36}$$

$$Cvs_{kj}^{a,(it)} = \begin{cases} vs_{kj}^{\phi_k,(it-1)} + vs_{kj}^{\phi_j,(it-1)} - 2vs_{kj} & a = DN \\ vs_{kj} - vs_{kj}^{DN,(it)} & otherwise \end{cases} \tag{37}$$

From the agent $a$ point of view, $PQ_{kj}^{(h)}$ is the results of $PQ_{kj}$ in iteration $h$, which is calculated by its neighboring agent through tie-branch $kj$. In the proposed MLATC approach, $h$ is related to the agent's levels. $h$ is equal to $it - 1$ when $le_{kj}^{a} > le^{a}$, and $le_{kj}^{a}$ is the level of the agent which is connected to agent $a$ through tie-branch $kj$. Also, if agent $a$ and its neighboring agent are at the same level ($le_{kj}^{a} = le^{a}$) and the neighbor's sublevel ($sl_{kj}^{a}$) is greater than agent $a$, $h$ is equal to $it - 1$. In other cases, $h$ is equal to $it$. Note, $le$ and $sl$ respectively represent the level and sublevel of the agents.

In the proposed MLATC framework, the agents on each side of tie-branch $kj$ share the voltage status with DN. So, two responses related to both sides of the tie-branch $kj$ are received by DN, while other agents receive only one target from DN, which is represented by (37). Note that $\phi_k$ and $\phi_j$ denote the agents on side $k$ and $j$ of the tie-branch $kj$, respectively.

In the proposed MLATC's iterative process, Lagrangian multipliers and penalty weights are updated at each iteration as follows:

$$Vpq_{kj}^{a,(it+1)} = Vpq_{kj}^{a,(it)} + 2Wpq_{kj}^{a,(it)} \circ Wpq_{kj}^{a,(it)} \circ Cpq_{kj}^{a,*(it)} \tag{38}$$

$$Vvs_{kj}^{a,(it+1)} = Vvs_{kj}^{a,(it)} + 2Wvs_{kj}^{a,(it)} \circ Wvs_{kj}^{a,(it)} \circ Cvs_{kj}^{a,*(it)} \tag{39}$$

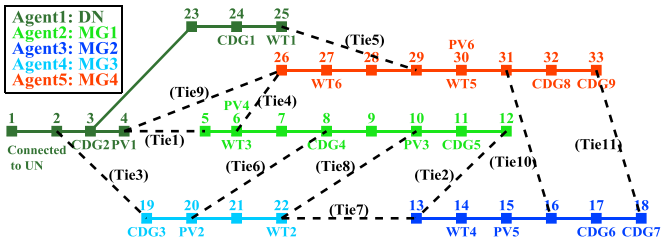


**Fig. 3.** The modified IEEE 33-bus network.

$$Wpq_{kj,z}^{a,(it+1)} = \begin{cases} Wpq_{kj,z}^{a,(it)} & \left|Cpq_{kj,z}^{a,*(it)}\right| \le \gamma \left|Cpq_{kj,z}^{a,*(it-1)}\right| \\ \beta \times Wpq_{kj,z}^{a,(it)} & \left|Cpq_{kj,z}^{a,*(it)}\right| > \gamma \left|Cpq_{kj,z}^{a,*(it-1)}\right| \end{cases} \forall z \in [1, ..., 2N] \tag{40}$$

$$Wvs_{kj,z}^{a,(it+1)} = \begin{cases} Wvs_{kj,z}^{a,(it)} & \left|Cvs_{kj,z}^{a,*(it)}\right| \le \gamma \left|Cvs_{kj,z}^{a,*(it-1)}\right| \\ \beta \times Wvs_{kj,z}^{a,(it)} & \left|Cvs_{kj,z}^{a,*(it)}\right| > \gamma \left|Cvs_{kj,z}^{a,*(it-1)}\right| \end{cases} \forall z \in [1, ..., N] \tag{41}$$

where $Cpq_{kj,z}^{a,*(it)}$ and $Cvs_{kj,z}^{a,*(it)}$ are the results of $Cpq_{kj,z}^{a,(it)}$ and $Cvs_{kj,z}^{a,(it)}$ which are calculated by agent $a$, respectively. $\beta$ and $\gamma$ are ATC parameters. To achieve the converged optimal results, $\beta$ should be greater than one ($\beta > 1$), and $\gamma$ can continually be selected from 0 to 1 ($0 < \gamma < 1$) [31].

As can be seen in (32) to (41), each agent only needs its local data and its related shared variables to solve its LSM. Accordingly, only shared variables should be visible and no further data of other agents need to be shared. This indicates that information privacy is properly addressed in the proposed MLATC-based framework.

The steps of the proposed MLATC-based framework are presented in Algorithm 1.

**Algorithm 1** The proposed MLATC framework.

1) Calculate all possible loops of the ADN ($L$). Define the level ($le^a$) and sublevel ($sl^a$) of agents. Set the initial value of shared variables, Lagrangian multipliers, and penalty weights. Set $it = 0$ and $le = 1$.

***While*** $\| C_{pq}^{*(it)}, C_{vs}^{*(it)} \|_{\max}$ do

2) Set $it = it + 1$.

3) Determine $Cpq_{kj}^{a,(it)}$ and $Cvs_{kj}^{a,(it)}$ by (36)-(37).

***For*** $le$=1 to $N^{le}$

4) The agents at level $le$ sequentially solve their LSM according to (32) in order of their sublevels ($sl$) and broadcast the result of their shared variables.

End of ***For***.

5) Update Lagrangian multipliers and penalty weights according to (38)-(41).

End of ***While***

**6)** Print the results.

Where $C_{pq}^{*(it)}$ and $C_{vs}^{*(it)}$ are two vectors that respectively represent the gap between results of active and reactive power flow and the gap between results of voltage status of all tie branches in all time intervals. $\| C_{pq}^{*(it)}, C_{vs}^{*(it)} \|_{max}$ shows the maximum gap between all the shared variables in the iteration $it$, and $\varepsilon$ is the convergence threshold. Note, the initial values of Lagrangian multipliers and penalty weights can be set arbitrarily in an acceptable range [31]. The initial values of voltage status can be set in the interval [0 $v_{max}{}^2$]. Also, the initial values of transacted active and reactive powers can be set arbitrary in the allowable range, i.e., from zero to the nominal capacity of tie branches.

## 5. Simulation results

To validate the scalability and accuracy of the proposed method, two test systems, i.e., the modified IEEE 33-bus and IEEE 123-bus distribution networks are considered as case studies.

**Table 1**
Rated power of PVs and WTs in the modified IEEE 33-bus network.

| WT generation (kW) | PV generation (kW) | Name |
|---|---|---|
| 25 | 100 | PV1/WT1 |
| 25 | 50 | PV2/WT2 |
| 50 | 50 | PV3/WT3 |
| 50 | 20 | PV4/WT4 |
| 25 | 20 | PV5/WT5 |
| 25 | 30 | PV6/WT6 |

**Table 2**
Data of CDGs in the modified IEEE 33-bus network.

| CDG | $P_{g_{\min},g}^{a}(kW)$ | $P_{g_{\max},g}^{a}(kW)$ | $a_g^a\left(\frac{S}{kW^2h}\right)$ | $b_g^a\left(\frac{S}{kWh}\right)$ | $c_g^a\left(\frac{S}{h}\right)$ |
|---|---|---|---|---|---|
| CDG 1 | 0 | 1000 | 0.0003 | 0.47 | 0 |
| CDG 2 | 0 | 800 | 0.0004 | 0.62 | 0 |
| CDG 3 | 0 | 500 | 0.0002 | 0.78 | 0 |
| CDG 4 | 0 | 500 | 0.0005 | 0.51 | 0 |
| CDG 5 | 0 | 800 | 0.0003 | 0.25 | 0 |
| CDG 6 | 0 | 1000 | 0.0001 | 0.18 | 0 |
| CDG 7 | 0 | 1000 | 0.0001 | 0.19 | 0 |
| CDG 8 | 0 | 2000 | 0.0001 | 0.11 | 0 |
| CDG 9 | 0 | 2000 | 0.0001 | 0.11 | 0 |

**Table 3**
Data of added tie branches in the modified IEEE 33-bus network.

| Tie no. | From | To | R(Ohm) | X(Ohm) |
|---|---|---|---|---|
| Tie5 | 25 | 29 | 0.12 | 0.12 |
| Tie6 | 20 | 8 | 0.2 | 0.28 |
| Tie7 | 22 | 13 | 0.1 | 0.15 |
| Tie8 | 22 | 10 | 0.75 | 0.85 |
| Tie9 | 4 | 26 | 0.11 | 0.15 |
| Tie10 | 31 | 16 | 0.12 | 0.25 |
| Tie11 | 33 | 18 | 0.1 | 0.25 |

All simulations have been conducted on a 3.20 GHz Intel Core i5-3470 CPU computer with 4 GB of RAM, using the YALMIP toolbox [32] in MATLAB R2019a and MOSEK v7.1.0.42 [33] solver. Note that the associated memory of each agent is not shared with other agents. In other words, the simulations are performed in such a way that agents cannot access the private data of each other.

### 5.1. The modified IEEE 33-bus network

The proposed decentralized framework is applied to the modified IEEE 33-bus distribution system shown in Fig. 3. This reconfigurable ADN contains 5 agents with 6 PVs, 6 WTs, and 9 CDGs. To distinguish agents, they are shown with a different color. The network data, as well as load data, can be found in [34], and the forecasted generation of PVs and WTs are given in Table 1. Also, the CDGs and added tie branches data are presented in Table 2 and Table 3, respectively. Before the optimization, it is assumed that all the lines are closed, then, the adjacency matrix of the network graph is built.

And the loop detection approach is executed using the depth-first search-based strategy. As it is presented in Table 4, 75 loops can be created through tie branches. For example, loop 1 is formed when all tie branches 1, 2, 7, and 3 are in service.

Using a cold start initialization strategy for the simulations, the initial values for targets/responses are set to zero. In the initial network configuration, it is assumed that the tie branches 1 to 4 are in service and the remaining tie branches are out of service. Accordingly, the voltage status values of tie branches 1 to 4 are initialized to 1 p.u., and the rest are initialized to 0. Also, the initial values of exchanged active and reactive power between agents are set to 0. The initial values of penalty weights and Lagrange multipliers variables are set to 1 and 0, respectively. Furthermore, the values of $\beta$, $\gamma$ and $\varepsilon$ are set to 1.01, 0.90, and

**Table 4**
Set of all loops created through tie branches (set $L$) in the modified IEEE 33-bus network.

| Loops 1–15 | Loops 16–30 | Loops 31–45 | Loops 46–60 | Loops 61–75 |
|---|---|---|---|---|
| [1,2,7,3] | [9,10,2,8,3] | [5,10,7,8,6,3] | [9,4,2,11,5] | [1,6,7,11,9] |
| [1,8,3] | [9,10,7,8,6,3] | [5,10,7,3] | [9,4,2,10,5] | [1,6,7,10,9] |
| [1,6,3] | [9,10,7,3] | [5,11,2,6,3] | [9,4,8,7,11,5] | [1,4,9] |
| [1,4,10,2,6,3] | [9,11,2,6,3] | [5,11,2,8,3] | [9,4,8,7,10,5] | [2,11,4] |
| [1,4,10,2,8,3] | [9,11,2,8,3] | [5,11,7,8,6,3] | [9,4,6,8,2,11,5] | [2,10,4] |
| [1,4,10,7,8,6,3] | [9,11,7,8,6,3] | [5,11,7,3] | [9,4,6,8,2,10,5] | [8,7,11,4] |
| [1,4,10,7,3] | [9,11,7,3] | [1,2,10,5] | [9,4,6,7,11,5] | [8,7,10,4] |
| [1,4,11,2,6,3] | [5,9,1,2,7,3] | [1,2,11,5] | [9,4,6,7,10,5] | [6,8,2,11,4] |
| [1,4,11,2,8,3] | [5,9,1,8,3] | [1,8,7,11,5] | [9,5] | [6,8,2,10,4] |
| [1,4,11,7,8,6,3] | [5,9,1,6,3] | [1,8,7,10,5] | [1,2,11,9] | [6,7,11,4] |
| [1,4,11,7,3] | [5,4,2,7,3] | [1,6,8,2,11,5] | [1,2,10,9] | [6,7,10,4] |
| [9,4,2,7,3] | [5,4,8,3] | [1,6,8,2,10,5] | [1,8,7,11,9] | [2,7,6] |
| [9,4,8,3] | [5,4,6,3] | [1,6,7,11,5] | [1,8,7,10,9] | [8,6] |
| [9,4,6,3] | [5,10,2,6,3] | [1,6,7,10,5] | [1,6,8,2,11,9] | [2,7,8] |
| [9,10,2,6,3] | [5,10,2,8,3] | [1,4,5] | [1,6,8,2,10,9] | [11,10] |

**Table 5**
Energy transaction between the agents in Case I.

| | | Receiving agents | | | | |
|---|---|---|---|---|---|---|
| | | DN | $MG_1$ | $MG_2$ | $MG_3$ | $MG_4$ |
| Sending agents | DN | – | -1358.4 | 0 | 285.6 | 0 |
| | $MG_1$ | 1358.5 | – | -648.9 | 0 | -1271.7 |
| | $MG_2$ | 0 | 648.9 | – | 0 | 0 |
| | $MG_3$ | -285.6 | 0 | 0 | – | 0 |
| | $MG_4$ | 0 | 1271.6 | 0 | 0 | – |

Note: "-" refers to importing power.

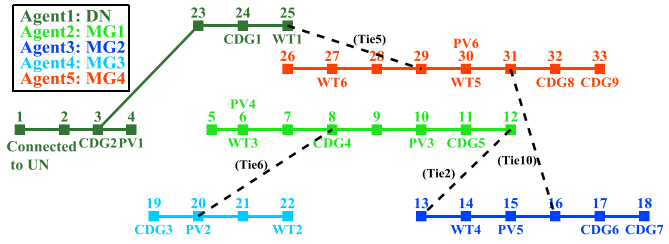


**Fig. 4.** Optimal configuration of the ADN in Case II.

0.0001 p.u., respectively. The forecasted wholesale market price is considered as 0.3808 $/kWh. The values of $SW^{a}_{max}$ and $c_{sw}$ are set to 6 and 0.001, respectively. Note that, $c_{sw}$ is assumed to be trivial to highlight the effect of reconfiguration on MGs energy trading.

To show the effectiveness of the proposed decentralized framework the following cases are studied:

Case I: No reconfiguration.

Case II: Reconfiguration with 8 tie-branch switching.

Case III: Reconfiguration by switching all tie branches.

Case IV: Increasing the number of agents.

Case V: Comparison with the centralized approach

### 5.1.1. Case I

In this case, it is assumed that the configuration of the ADN is the same as the initial one, and tie-branch switching is not allowed. In this case, the proposed model converges after 34 iterations, and the total operation cost of ADN, i.e., operating costs of all agents, and total active power loss of the ADN are equal to 771.5 $ and 124 kW, respectively.

The exchanged energy among agents is given in Table 5. As it is evident, the neighboring agents are well converged on the same exchanged energy.

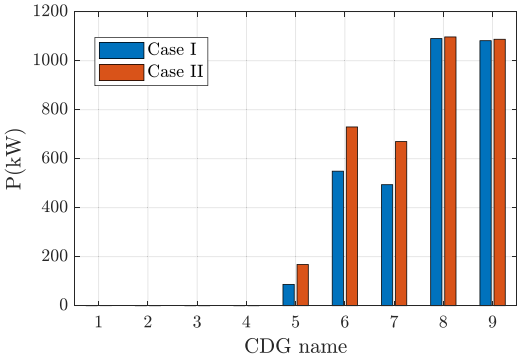


**Fig. 5.** Power generation of CDGs in Cases I and II.

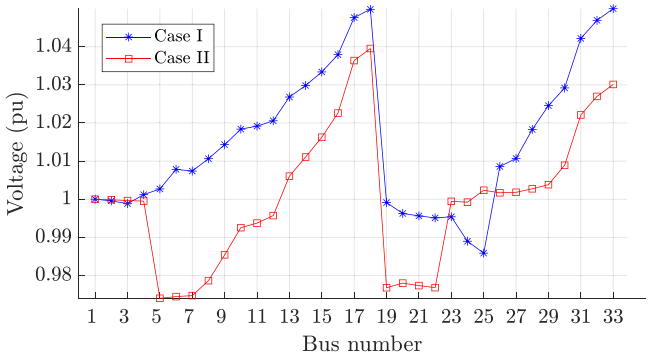


**Fig. 6.** Voltage profiles of Cases I and II.

### 5.1.2. Case II

All conditions in this scenario are like Case I, while the topology of the ADN can be optimized via switching of tie branches 1–6 and 10–11. Accordingly, the status of the tie branches 7–9 is forced to zero. The optimal configuration of the ADN is shown in Fig. 4.

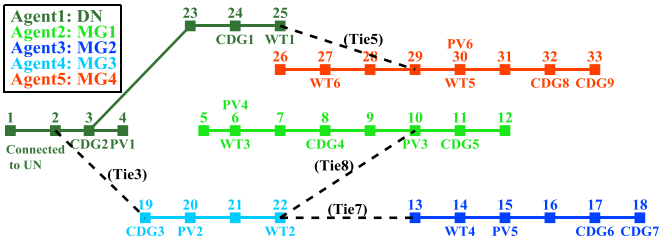


**Fig. 7.** Optimal configuration of the ADN in case III.

**Table 6**
Comparison of the results of Cases I, II, and III in the modified IEEE 33-bus network.

| Case | Cost ($) | Loss (kW) | Minimum voltage (pu) | Time (seconds) | Iteration |
|---|---|---|---|---|---|
| I | 771.5357 | 124.1161 | 0.9858 | 12.0039 | 34 |
| II | 739.3734 | 121.7710 | 0.9740 | 81.5633 | 68 |
| III | 723.6324 | 110.8479 | 0.9931 | 46.6785 | 21 |

As can be seen, tie branches 2, 5, 6, and 10 are in service; and the radiality of the ADN is preserved. Compared to Case I, the operating costs of all agents and the power losses of the ADN are decreased by $ 32.16 and 2.35 kW, respectively. As shown in Fig. 5, this is due to the increased generation of CDGs 5 to 9, which have a relatively low operating cost. The possibility of more generation by these resources was restricted in Case I due to the maximum voltage limitation of buses 18 and 33 (i.e., 1.05 p.u.) as depicted in Fig. 6. However, these limitations are eliminated via optimal tie-branch switching in Case II, and the power generation of these low-cost resources has increased.

### 5.1.3. Case III

In this case, switching of all the tie branches is allowed. The optimal configuration of the ADN is shown in Fig. 7. As it is evident, tie branches 3, 5, 7, and 8 are in service. The results of Cases I to III are compared in Table 6.

Although the solution time increases in Case III, it leads to minimum total operation cost and total losses and a smoother voltage profile of the ADN.

### 5.1.4. Case IV

To show the convergence of the proposed MLATC method, the number of agents is increased to 8 as depicted in Fig. 8.

To do so, some of the internal branches become tie branches and vice versa, and the size of the agents is considered greatly different. The optimal configuration of the ADN is presented in Fig. 9.

Moreover, the convergence of the proposed MLATC in cases III and IV are plotted in Fig. 10. As it is evident, the proposed model converges after 40 iterations when the number of agents is increased to 8.

### 5.1.5. Case V

To show the optimality and effectiveness of the proposed MLATC method, the results of all previous cases are compared with the centralized approach.

To do so, all agents should send their private information, i.e., DERs, local loads data, to DSO. Then, DSO centrally schedules all resources and sends the related results to every agent. Although the centralized method violates the privacy and autonomy of the agents, it can reach the optimal solution and can be a good criterion to evaluate the optimality of the obtained results of the proposed model.

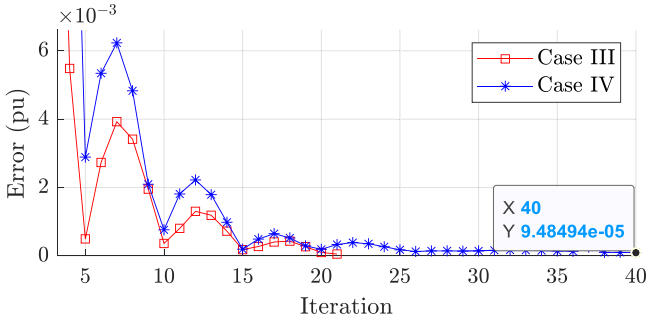


**Fig. 10.** Convergence performance of the proposed method in the modified IEEE 33-bus network.

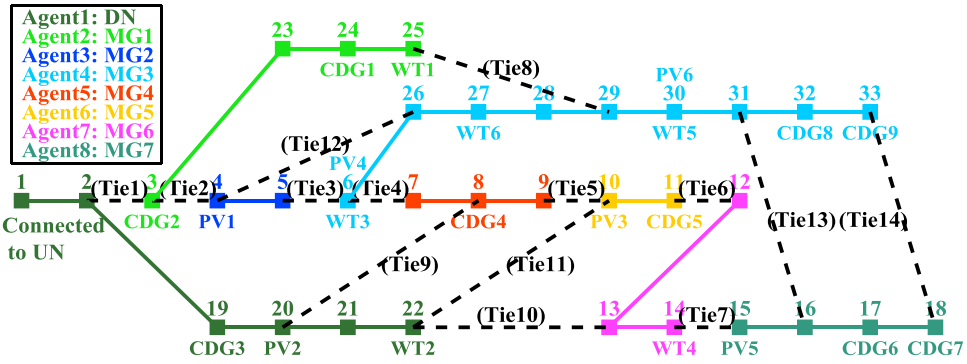


**Fig. 8.** Modified reconfigurable IEEE 33-bus network with 8 agents (Case IV).

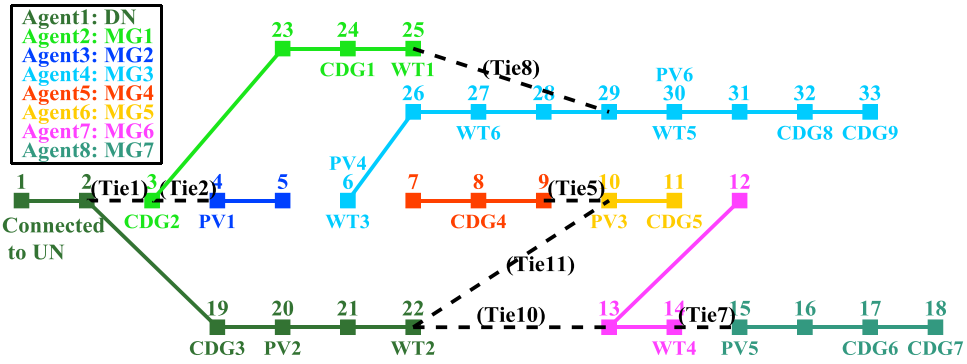


**Fig. 9.** Optimal configuration of the ADN in Case IV.

**Table 7**
Comparison of the results of the centralized and the proposed MLATC approaches in the modified IEEE 33-bus network.

| Case | Approach | CPU time (second) | Required iteration | Total cost of ADN ($) | Gap (%) |
|---|---|---|---|---|---|
| I | MLATC | 12.00 | 34.00 | 771.54 | 0.06 |
| | Centralized | 1.32 | - | 772.03 | |
| II | MLATC | 81.56 | 68.00 | 739.37 | 0.00 |
| | Centralized | 42.89 | - | 739.35 | |
| III | | 46.68 | 21.00 | 723.63 | 0.00 |
| | MLATC | | | | |
| | Centralized | 45.23 | - | 723.64 | |
| 1v | MLATC | 144.83 | 40.00 | 723.67 | 0.01 |
| | Centralized | 233.73 | - | 723.60 | |

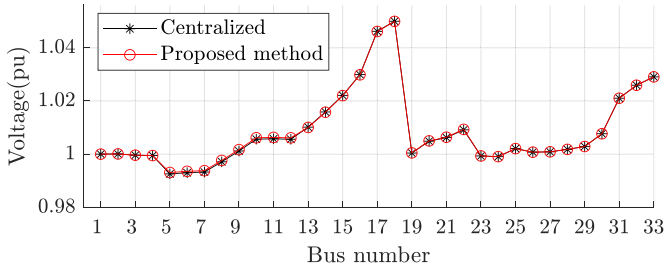


**Fig. 11.** Voltage profile comparison of Case III.

According to Table 7, the proposed decentralized framework converged to optimal solutions with an acceptable gap, less than 0.07%, in all cases, while it preserves the autonomy and privacy of all agents. Moreover, the CPU time of both proposed and centralized methods is increased when the number of tie branches and agents is grown.

However, the CPU time of the proposed method is almost 62% of the centralized method in Case IV. It clearly shows that the proposed method is fast and scalable and can be easily applied for the short-term operation of the ADN. Also, the voltage profile of Case III is depicted in Fig. 11 to show how similar the power flow results are in both centralized and proposed MLATC methods.

### 5.2. The modified IEEE 123-bus network

The proposed MLATC framework is applied to the modified IEEE 123-bus distribution network to determine its optimal day-ahead scheduling.

As shown in Fig. 12, this ADN contains 123 nodes, 118 internal branches, and 5 agents, i.e., DN, and MG1 to MG4. These agents can be interconnected through 6 tie branches, i.e., Tie1 to Tie6. Peak load and branch data are given from [35]. However, all data of this ADN is available online [36].

When all tie branches are in service, 3 loops $Lp_1 = \{1,2,6,3,5,4\}$, $Lp_2 = \{1,2,6,4\}$, and $Lp_3 = \{3,5\}$ can be created. Since loop 3 ($Lp_3$) contains only two tie branches, Tie3 and Tie5, it is expected that in each time interval, only one of them is in service.

It is assumed that the scheduling horizon is 24 h, i.e., $T = \{1,\ldots,24\}$. The forecasted values of the load, renewable production, and price profiles are shown in Fig. 13.

Both the centralized and the proposed MLATC are applied to this ADN. The convergence curve of the proposed MLATC is shown in Fig. 14. As can be seen, it converges at iteration 47.

The CPU time and cost of the ADN are summarized in Table 8.

As it is evident, the CPU time of the proposed MLATC is significantly less than the CPU time of the centralized approach. This originates from the decentralized nature of the proposed method. The centralized model is much more complicated than the LSM of each agent. The gap between the total cost of the ADN with centralized and the proposed MLATC methods is less than 0.23%, which satisfies the accuracy of the proposed MLATC method. In this ADN the total cost of the ADN is negative due to the high penetration level of renewable resources. It means that the ADN sells surplus power generation of its renewables to the UN. The imported power from the UN in all time intervals is shown in Fig. 15.

In all time intervals, except $t = 3$, 5–7, and 17–20 (when the PVs generation are zero), the imported power from the UN ($Pun_t^a$) is negative. As can be seen, the results of both the centralized and the MLATC approaches are the same.

In Fig. 16, the voltage status of all tie branches is shown. As expected, Tie3 and Tie5 are not simultaneously switched on. From $t = 1$ to $t = 13$, Tie3 is in service, while Tie5 is switched on in other intervals, i.e., from $t = 14$ to $t = 24$. However, Tie1, Tie2, and Tie4 are permanently in

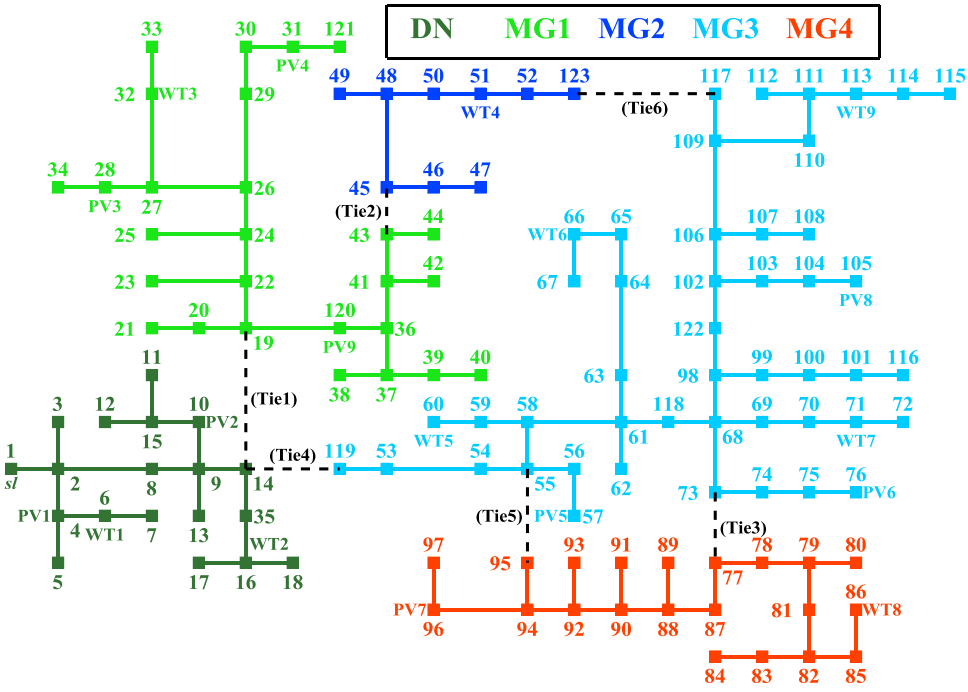


**Fig. 12.** The modified IEEE 123-bus distribution network.

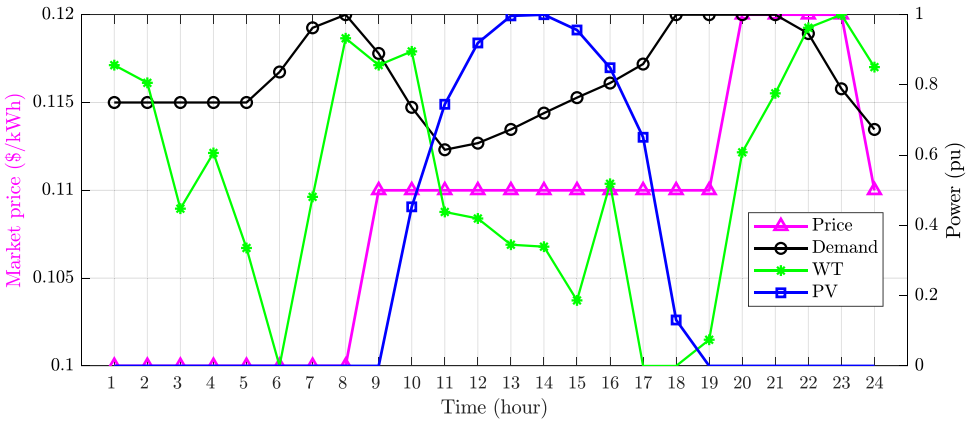


**Fig. 13.** Daily load profile [37] (peak load is limited to 1 pu), renewable generation [8], and wholesale market price forecast [38] for the modified IEEE 123-bus network.

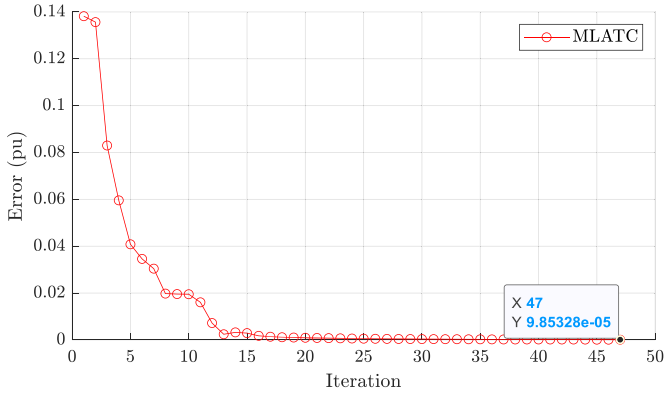


**Fig. 14.** Convergence performance of the proposed method in the modified IEEE 123-bus network.

**Table 8**
Comparison of the results of the centralized and proposed MLATC methods for the modified IEEE 123-bus network.

| Approach | CPU time (second) | Iteration | Total cost of the ADN ($) | Gap (%) |
|---|---|---|---|---|
| Centralized | 801.06 | – | -3194.5 | 0.23 |
| MLATC | 661.17 | 47 | -3187.2 | |

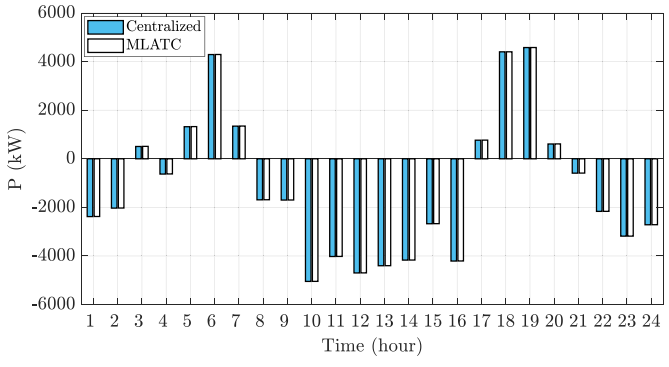


**Fig. 15.** Imported active power from the UN in the modified IEEE 123-bus network.

service, while Tie6 is always switched off (its voltage status is zero). These results confirm the realization of radiality constraint (23) in the decentralized style.

Finally, the nodal voltage magnitude of all buses is shown in Fig. 17. As can be seen, all nodal voltages are in allowable limits, which satisfy constraint (15). Note, the minimum voltage magnitude of this AND ($v_{min}$) is set to 0.9 pu, while its upper limit ($v_{max}$) is 1.05 pu.

## 6. Conclusion

In this paper, a novel decentralized framework was presented to schedule a reconfigurable ADN with multiple autonomous MGs. In the proposed framework, a decentralized AC load flow model was developed to fully address the network constraints and the potential physical connection between two neighboring agents. Also, a new MLATC-based method was proposed to provide coordination among agents while preserving their autonomy and information privacy. In the proposed MLATC framework, each agent locally operates its internal network and resources, and only an iterative process with limited data sharing is required. Several case studies on the modified IEEE 33-bus and IEEE 123-bus networks demonstrated that: (1) Optimal reconfiguration of the ADN can effectively reduce the overall operation costs and active power losses of ADN via optimal energy trading among agents, and can improve the security of the network. (2) The proposed model can successfully converge to the optimal scheduling of agents in a limited number of iterations. (3) The proposed method is fast and scalable. Therefore, it can well be applied for the short-term operation of the ADN with multiple autonomous MGs.

In this paper, it is assumed that the ADN is balanced. However, real distribution networks may also include unbalanced situations. Therefore, optimal decentralized scheduling of a reconfigurable ADN with a high-penetration level of single-phase loads and DERs can be considered for future work. Also, developing a parallel decentralized optimization method, in which the agents can simultaneously solve their LSMs, may speed up the scheduling problem.

## CRediT authorship contribution statement

**Houman Bastami:** Conceptualization, Methodology, Software, Writing – original draft, Formal analysis, Investigation, Visualization. **Mahmoud Reza Shakarami:** Project administration, Writing – review & editing, Validation, Investigation, Resources, Supervision. **Meysam Doostizadeh:** Data curation, Conceptualization, Visualization, Writing – review & editing, Validation, Formal analysis.

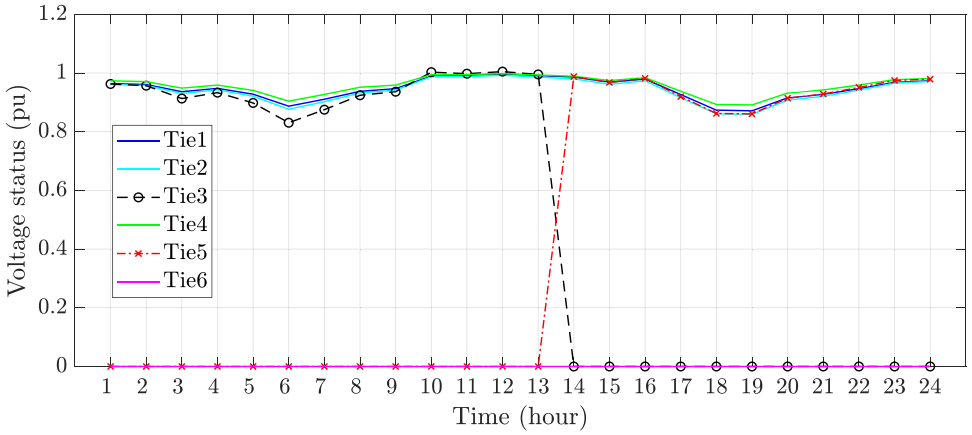


**Fig. 16.** Voltage status of all tie branches in the modified IEEE 123-bus network.

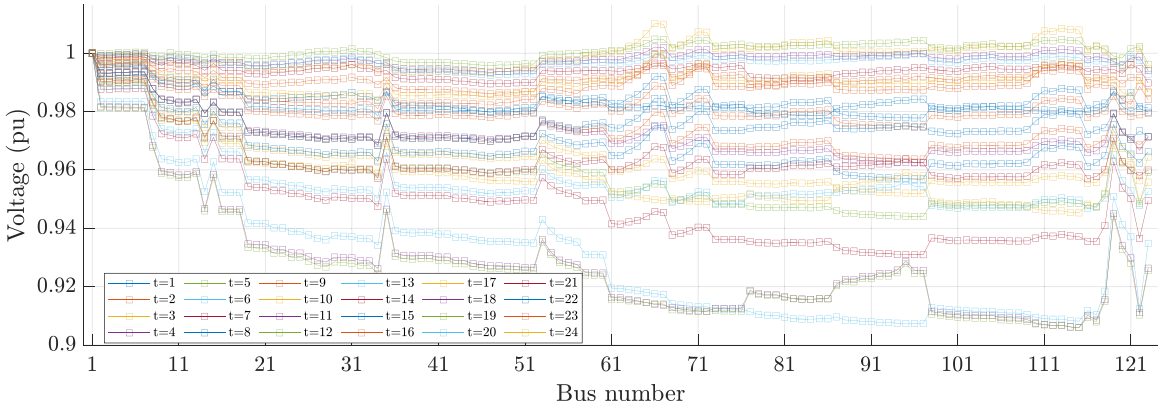


**Fig. 17.** Voltage profiles of the modified IEEE 123-bus network in all time intervals.

## Declaration of Competing Interest

The authors declare that they have no known competing financial interests or personal relationships that could have appeared to influence the work reported in this paper.

## References

[1] J. Hu, H. Cong, C. Jiang, Coordinated scheduling model of power system with active distribution networks based on multi-agent system, J. Mod. Power Syst. Clean Energy 6 (2018) 521–531, https://doi.org/10.1007/s40565-017-0327-7.

[2] Z. Wang, B. Chen, J. Wang, J. kim, Decentralized energy management system for networked microgrids in grid-connected and islanded modes, IEEE Trans. Smart Grid 7 (2016) 1097–1105, https://doi.org/10.1109/TSG.2015.2427371.

[3] D. Zhu, B. Yang, Q. Liu, K. Ma, S. Zhu, C. Ma, et al., Energy trading in microgrids for synergies among electricity, hydrogen and heat networks, Appl. Energy 272 (2020), 115225, https://doi.org/10.1016/j.apenergy.2020.115225.

[4] M. Doostizadeh, H. Ghasemi, Day-ahead scheduling of an active distribution network considering energy and reserve markets, Int. Trans. Electr. Energy Syst. 23 (2013) 930–945, https://doi.org/10.1002/etep.1630.

[5] A. Borghetti, M. Bosetti, S. Grillo, S. Massucco, C.A. Nucci, M. Paolone, et al., Short-term scheduling and control of active distribution systems with high penetration of renewable resources, IEEE Syst. J. 4 (2010) 313–322, https://doi.org/10.1109/JSYST.2010.2059171.

[6] A. Saint-Pierre, P. Mancarella, Active distribution system management: a dual-horizon scheduling framework for DSO/TSO interface under uncertainty, IEEE Trans. Smart Grid 8 (2017) 2186–2197, https://doi.org/10.1109/TSG.2016.2518084.

[7] J.F. Franco, M.J. Rider, M. Lavorato, R. Romero, A mixed-integer LP model for the reconfiguration of radial electric distribution systems considering distributed generation, Electr. Power Syst. Res. 97 (2013) 51–60, https://doi.org/10.1016/j.epsr.2012.12.005.

[8] M. Doostizadeh, M.R. Shakarami, H. Bastami, Decentralized energy trading framework for active distribution networks with multiple microgrids under uncertainty(Invited Paper), Sci. Iran. 26 (2019) 3606–3621, https://doi.org/10.24200/sci.2019.53962.3557.

[9] A.K. Marvasti, Y. Fu, S. DorMohammadi, M. Rais-Rohani, Optimal operation of active distribution grids: a system of systems framework, IEEE Trans. Smart Grid 5 (2014) 1228–1237, https://doi.org/10.1109/TSG.2013.2282867.

[10] C. Feng, F. Wen, L. Zhang, C. Xu, M.A. Salam, S. You, Decentralized energy management of networked microgrid based on alternating-direction multiplier method, Energies 11 (2018) 2555, https://doi.org/10.3390/en11102555.

[11] W. Zheng, W. Wu, B. Zhang, H. Sun, Y. Liu, A fully distributed reactive power optimization and control method for active distribution networks, IEEE Trans. Smart Grid 7 (2016) 1021–1033, https://doi.org/10.1109/TSG.2015.2396493.

[12] S. Esmaeili, A. Anvari-Moghaddam, S. Jadid, Optimal operational scheduling of reconfigurable multi-microgrids considering energy storage systems, Energies 12 (2019) 1766, https://doi.org/10.3390/en12091766.

[13] Y. Wang, Z. Huang, M. Shahidehpour, L.L. Lai, Z. Wang, Q. Zhu, Reconfigurable distribution network for managing transactive energy in a multi-microgrid system, IEEE Trans. Smart Grid 11 (2020) 1286–1295, https://doi.org/10.1109/TSG.2019.2935565.

[14] H. Bastami, M.R. Shakarami, M. Doostizadeh, A non-hierarchical ATC framework for parallel scheduling of active distribution network with multiple autonomous microgrids, Int. J. Electr. Power Energy Syst. 133 (2021), 107293, https://doi.org/10.1016/j.ijepes.2021.107293.

[15] A. Kargarian, J. Mohammadi, J. Guo, S. Chakrabarti, M. Barati, G. Hug, et al., Toward distributed/decentralized DC optimal power flow implementation in future electric power systems, IEEE Trans. Smart Grid 9 (2016) 2574–2594, https://doi.org/10.1109/TSG.2016.2614904.

[16] E. Kazemi-Robati, M.S. Sepasian, Passive harmonic filter planning considering daily load variations and distribution system reconfiguration, Electr. Power Syst. Res. 166 (2019) 125–135, https://doi.org/10.1016/j.epsr.2018.09.019.

[17] C. Li, S. Miao, Y. Li, D. Zhang, C. Ye, Z. Liu, et al., Coordinating Dynamic Network Reconfiguration with ANM in active Distribution Network Optimization Considering System Structure Security Evaluation, 13, IET Generation, Transmission & Distribution, 2019, pp. 4355–4363. Available: https://digital-li

brary.theiet.org/content/journals/10.1049/iet-gtd.2018.6583.
[18] S. Chen, W. Hu, Z. Chen, Comprehensive cost minimization in distribution networks using segmented-time feeder reconfiguration and reactive power control of distributed generators, IEEE Trans. Power Syst. 31 (2016) 983–993, https://doi.org/10.1109/TPWRS.2015.2419716.
[19] M. Abdelaziz, Distribution network reconfiguration using a genetic algorithm with varying population size, Electr. Power Syst. Res. 142 (2017) 9–11, https://doi.org/10.1016/j.epsr.2016.08.026.
[20] H. Karimianfard, H. Haghighat, An initial-point strategy for optimizing distribution system reconfiguration, Electr. Power Syst. Res. 176 (2019), 105943, https://doi.org/10.1016/j.epsr.2019.105943.
[21] R. Pegado, Z. Naupari, Y. Molina, C. Castillo, Radial distribution network reconfiguration for power losses reduction based on improved selective BPSO, Electr. Power Syst. Res. 169 (2019) 206–213, https://doi.org/10.1016/j.epsr.2018.12.030.
[22] M. Hemmati, B. Mohammadi-Ivatloo, S. Ghasemzadeh, E. Reihani, Risk-based optimal scheduling of reconfigurable smart renewable energy based microgrids, Int. J. Electr. Power Energy Syst. 101 (2018) 415–428, https://doi.org/10.1016/j.ijepes.2018.04.005.
[23] Z. Tian, W. Wu, B. Zhang, A. Bose, Mixed-Integer second-order cone Programing model for VAR Optimization and Network Reconfiguration in Active Distribution Networks, 10, IET Generation, Transmission & Distribution, 2016, pp. 1938–1946. Available, https://digital-library.theiet.org/content/journals/10.1049/iet-gtd.2015.1228.
[24] S. Golshannavaz, S. Afsharnia, F. Aminifar, Smart distribution grid: optimal day-ahead scheduling with reconfigurable topology, IEEE Trans. Smart Grid 5 (2014) 2402–2411, https://doi.org/10.1109/TSG.2014.2335815.
[25] S. Esmaeili, A. Anvari-Moghaddam, S. Jadid, J.M. Guerrero, A stochastic model predictive control approach for joint operational scheduling and hourly reconfiguration of distribution systems, Energies 11 (2018) 1884, https://doi.org/10.3390/en11071884.
[26] B. Zeng, J. Shi, J. Wen, J. Zhang, A game-theoretic framework for active distribution network planning to benefit different participants under the electricity market, Turk. J. Electr. Eng. Comput. Sci. 25 (2017) 83–94, https://doi.org/10.3906/elk-1504-94.
[27] M. Farivar, S.H. Low, Branch flow model: relaxations and convexification—part I, IEEE Trans. Power Syst. 28 (2013) 2554–2564, https://doi.org/10.1109/TPWRS.2013.2255317.
[28] B. Moradzadeh, "Optimal Distribution Reconfiguration and Demand Management within Practical Operational Constraints, University of Tennessee, 2013. Ph.D. https://trace.tennessee.edu/utk_graddiss/2464.
[29] A. Akrami, M. Doostizadeh, F. Aminifar, Optimal reconfiguration of distribution network using $\mu$ PMU measurements: a data-driven stochastic robust optimization, IEEE Trans. Smart Grid 11 (2020) 420–428, https://doi.org/10.1109/TSG.2019.2923740.
[30] S. Tosserams, L. Etman, P. Papalambros, J. Rooda, An augmented Lagrangian relaxation for analytical target cascading using the alternating direction method of multipliers, Struct. Multidiscip. Optim. 31 (2006) 176–189, https://doi.org/10.1007/s00158-005-0579-0.
[31] Y. Jung, N. Kang, I. Lee, Modified augmented Lagrangian coordination and alternating direction method of multipliers with parallelization in non-hierarchical analytical target cascading, Struct. Multidiscip. Optim. 58 (2018) 555–573, https://doi.org/10.1007/s00158-018-1907-5.
[32] J. Lofberg, YALMIP: a toolbox for modeling and optimization in MATLAB, in: Proceedings of the IEEE International Conference on Robotics and Automation (IEEE Cat. No.04CH37508), 2004, pp. 284–289, https://doi.org/10.1109/CACSD.2004.1393890, 2004.
[33] A. Mosek, "The MOSEK optimization software," Online at http://www.mosek.com, vol. 54, p. 5, 2010.
[34] M.E. Baran, F.F. Wu, Network reconfiguration in distribution systems for loss reduction and load balancing, IEEE Trans. Power Deliv. 4 (1989) 1401–1407, https://doi.org/10.1109/61.25627.
[35] X. Chen, W. Wu, B. Zhang, Robust restoration method for active distribution networks, IEEE Trans. Power Syst. 31 (2016) 4005–4015, https://doi.org/10.1109/TPWRS.2015.2503426.
[36] (2021). Data of the modified IEEE 123-bus distribution network. Available: https://drive.google.com/file/d/1-dNDAKkn2pGD0r0z4ds_hZGUfmS7uO9K/view?usp=sharing.
[37] B.C. de Oliveira, J.L.R. Pereira, G. de O. Alves, I.D. Melo, M.A. de Souza, P.A. N. Garcia, Decentralized three-phase distribution system static state estimation based on phasor measurement units, Electr. Power Syst. Res. 160 (2018) 327–336, https://doi.org/10.1016/j.epsr.2018.03.010.
[38] Z. Ghofrani-Jahromi, M. Kazemi, M. Ehsan, Distribution switches upgrade for loss reduction and reliability improvement, IEEE Trans. Power Deliv. 30 (2015) 684–692, https://doi.org/10.1109/TPWRD.2014.2334645.